

Experimental Design with Integrated Temperature Sensors in MEMS: an Example of Application for Rarefied Gases

Alice VITTORIOSI ^{1*}, Juergen J. BRANDNER ¹, Roland DITTMAYER ¹

* Corresponding author: Tel.: ++49 (0)721 6082 8136; Fax: ++49 (0)721 6082 3186;
Email: alice.vittoriosi@kit.edu

1: Institute for Micro Process Engineering, Karlsruhe Institute of Technology, Germany

Abstract This paper presents a new MEMS experimental device with integrated temperature sensors. Conventional silicon planar techniques for the fabrication of microelectronic sensors have been used to realize a particular layout, which does not limit the material of the microstructures it can be used with. The study of rarefied gases has been chosen as case study for the validation of the local measuring system. In this work the attention will be focused on the description of the sensor functioning principles and on the presentation of the preliminary results obtained during the calibration procedures. The tests showed promising results for a future development of the sensor design.

Keywords: Integrated sensors, temperature measurements, gas flows, slip flow

1. Introduction

Micro electro mechanical systems (MEMS) are constantly developing as a new technological area which finds a variety of different applications and offers the possibility of achieving intensified and efficient processes. MEMS mainly rely on the use of structures which characteristic lengths fall below the millimeter range. Despite the huge advances in micro- and nano-manufacturing techniques, allowing the development of a number of sophisticated and miniaturized systems, many open questions are still present in understating the transport phenomena taking place in these devices. Many fundamental studies on microfluidics demonstrated the importance of considering effects such as compressibility, rarefaction and surface interactions, which may usually be negligible for conventional systems but acquire importance at the small scales (Guo and Li, 2003, Morini, 2004; Rosa, et al., 2008).

The identification of the governing physical mechanisms for microchannel systems requires on the one hand the development of theoretical models which include scaling effects and on the other hand the capability of acquiring experimental data showing these effects and validating the

theoretical models. This is important to optimize microstructured systems and provide reliable tools for MEMS design and performance prediction.

The scaling of measuring systems parallel to that of flow devices represents one of the possible methods to investigate micro flows. The miniaturization of sensors and transducers already began in the early '70s thanks to the development of silicon planar technology. These techniques allow the integration of detectors and sensors elements on small silicon chips. Van Oudheudsen (1989) developed a fully integrated flow sensor system based on microelectronic techniques. Shear stress sensors (Schmidt, et al., 1988), pressure transducers (Krause and Fralick, 1977) and temperature sensors (Van Herwaarden, et al., 1989) are other examples of application of miniaturized sensor designs for "large-scale" environments. Another appealing employment of such technology is the possibility of installing miniature transducers in microchannels. Such integrated systems require high frequency responses and high sensitivity since the quantities to be measured are smaller compared to conventional scales. Example of MEMS-based sensors in microchannels can be retrieved in some recent references. Wu et al. (1998) developed e.g. an

embedded silicon microchannel system with temperature sensors. Park et al. (2003) developed an integrated assembly with platinum RTD sensors on silicon microchannels bonded on a glass lid. Glass has also been employed by Xue and Qiu (2005) integrating an array of temperature sensors in a microchannel fabricated with planar fabrication techniques.

As can be noticed by these examples, silicon-based manufacturing techniques allow the miniaturization of sensing systems, but basically limit the employable structure materials to silicon and glass. However, many practical MEMS applications (when harsh working conditions are reached, or highly heat conductive materials are necessary) require the employment of different materials, i.e. metals, polymers and ceramics.

To allow a broad implementation if this technology more flexible designs are necessary. Ko and Gau (2009) presented recently an innovative low temperature manufacturing technique for the fabrication of polymeric microstructured channels with integrated sensors. However, even if this technique overcomes some of the typical limits of sensor integration in MEMS, the complexion of its realization and the specificity of its application make the use of this system difficult for extended practical tasks.

This paper presents the design and the implementation of an integrated miniaturized measuring system for MEMS, enabling the employment of different channel materials, which can be easily removed and changed. The measuring system has been developed parallel to an experimental setup for the characterization of gas flows in microchannels under rarefied conditions. This problem represents a typical example where a local flow characterization is necessary for a full understanding of the flow features and for these reasons it has been chosen as validation case study for the sensor prototypes. Nevertheless, as it will be demonstrated in the following sections, the present design can be easily adapted for a number of applications other than the single one described here,

making this system particularly appealing for future developments.

1.1 Gas flows under rarefied conditions

Gas flows in microchannels are often encountered in the so-called slip flow conditions, which refer to a non continuous behavior of the gas flow in proximity of the gas-wall interface (Gad-el-Hak, 2002). In particular, within few mean free paths away from the wall a slip velocity and a temperature jump can be found, which should be included in the flow modeling by modifying the boundary conditions of the Navier-Stokes equations (Colin, 2005). A useful parameter in the study of rarefied gases is the Knudsen number defined as the ratio between the molecule mean free path and the system characteristic length ($Kn \equiv \lambda / L$). The Knudsen number assesses the degree of deviations from the continuous approximation, and defines different rarefaction regimes (Beskok and Karniadakis, 1999).

As the discontinuities first appear near the wall, it is clear that the gas-surface interactions play a major role in determining the flow behavior in this region. Several experimental studies have been done to characterize gas flows in microchannels under slip flow (some examples can be found in Arkilic (1997), Turner (2004) and Pitakarnnop (2010)), but most of them are based on the indirect evaluation of the rarefaction parameters with measurements performed outside the channels or did not offer a complete overview of the flow characteristics. Even if these studies are useful for the validation of theoretical models, they do not help identifying the actual role of the surface interactions on the flow. This is a typical local scale phenomenon which requires direct measurements inside the channels and could therefore benefit of the measuring technique proposed in this work.

2. Experimental setup

The developed experimental setup allows the performance of heat transfer studies for gas flows in microchannels under varying working conditions and with different channel materials

and geometries. In particular a flexible layout has been developed which allows the variation of the test sections and of the boundary conditions, while keeping the same measuring system throughout all the experiments.

2.1 Experimental device

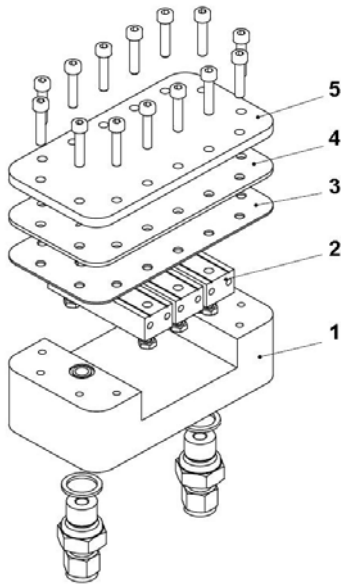


Fig. 1. Scheme of the multilayer experimental device with integrated measurements system (4) and exchangeable test sections (3).

The experimental device presents a multilayer configuration, where each layer covers a specific function and works independently from the others (Vittoriosi, et al., 2010). A schematic representation of the device is shown in Fig. 1. The device includes a heating/cooling unit, constituted by three thermally insulated copper blocks with receptacle holes for electrically powered heating elements or cooling loop tubes. The block temperature defines the thermal boundary conditions of the test sections and is monitored/controlled by thermocouples installed on top of the blocks. The thermal performances of a similar heating/cooling unit design have been previously investigated by Maikowske et al. (2010).

The upper layer constitutes the test section and consists of a foil where a three-wall channel open on the top is manufactured. The material of the foil can be chosen according to the case, as well as the manufacturing technique, and the test section can be easily

changed by disassembling and remounting the device.

The fourth and closing wall of the channel is constituted by the third layer, which also includes the integrated measuring system. The sensors are manufactured on a single silicon chip covering the entire channel length. In particular a series of temperature transducers have been realized on top of thin film membranes which faces the inner part of the channel and directly access information of the gas flow. Further details on the sensor design will be given in the next section. The sensor chip is installed on a PTFE support frame which also enables the sealing of the whole structure. Indeed, the elastic properties of the support material grant that, once the structure is closed, a direct contact between the PTFE and the channel foil is established, minimizing the gas leakages outside the channel. The sealing properties of the device have been verified with low pressure tests on the whole experimental circuit (including the auxiliary measuring system outside the device). Overall leakage rates of about $8 \cdot 10^{-2} \text{ mbar} \cdot \text{l} \cdot \text{sec}^{-1}$ have been measured. Finally, the structure is closed by simple clamping, which make possible the exchange of the test sections.

The device is installed into an experimental loop including a vacuum pump for the regulation of the rarefaction levels at the channel inlet and outlet and a complete measuring system to monitor the pressure and the temperature of the gas at the inlet and outlet of the device. To eliminate the influence of the thermal losses with the environment, the device is installed into a closed volume which can be evacuated during the heat transfer tests.

2.2. Integrated measuring system

A series of temperature sensors have been manufactured on a silicon substrate with planar microelectronic processes. The sensors present a thermopile configuration (van Herwaarden, 1989) which exploits the Seebeck thermoelectric effects like thermocouples, but, instead of a single junction, presents several junctions in parallel to increase the overall sensitivity. In the present case a ten junction design has been chosen with the two materials

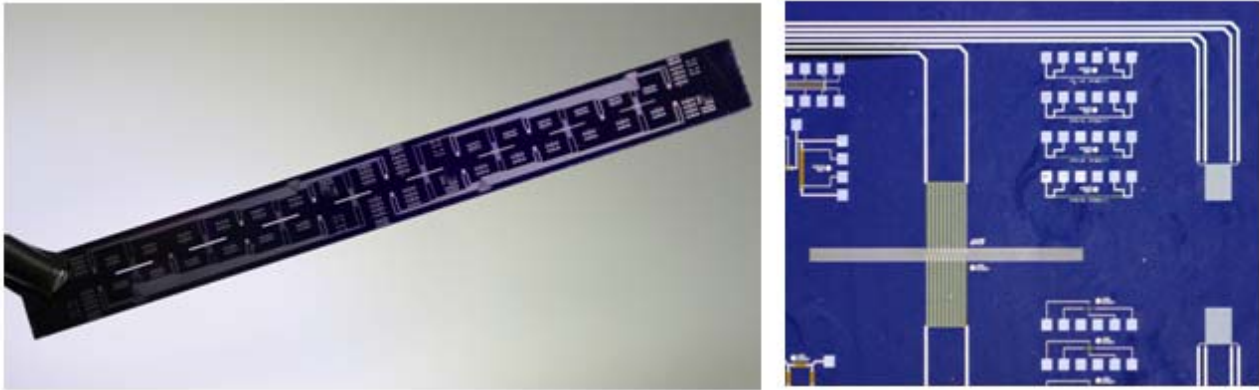


Fig. 2. Example of a manufactured chip (left) with an array of thin film membranes and detail of the sensors structures (right) with thermopiles on top of the membranes and RTD on the chip substrate.

being aluminum and n-doped polysilicon. To avoid thermal shortcuts (spoiling the sensor sensitivity), the sensors are fabricated on top of thin film membranes (10-15 μm thick) realized by a wet etching of the chip back side.

The thermopiles retrieve the temperature difference between the centerline of the membranes and the chip substrate (where the sensor contact leads end). As the membrane is in contact with the gas flow in the microchannel, the signal can be interpreted as the temperature difference between the gas and the chip. To retrieve the gas absolute temperature a reference signal is necessary. For this purpose, a series of RTD sensors with a four wires configuration have been realized on the chip, at the same positions of the thermopiles contact lead ends. The RTD signal is the absolute chip temperature (T_{chip}) and can be combined with the differential value measured by the thermopiles (ΔT_{gas}) to evaluate the gas absolute temperature (T_{gas}):

$$T_{gas} = T_{chip} \pm \Delta T_{gas} \quad (1)$$

The sign in equation (1) depends in the

specific problem (whether the gas flow is heated or cooled with respect to the chip substrate).

Figure 2 presents a picture of a realized chip with a detail of the thermopile/RTD system. The chip comprises 8 membranes 160 μm wide, each containing two thermopiles (one per side). This configuration allows a symmetric distribution of the heat conduction along the sensor leads and a redundant measure of the temperature at each position. Finally the chip contains 16 RTD sensors at different positions.

The data registered by the sensors are collected at the end of the contact leads on the chip sides. Here four polyimide flexible cables have been manufactured and bonded to transfer the data out of the device, where they are collected by a digital acquisition system.

The cable bonding is realized by a precision positioning of the two parts and by the application of a two-period pressure/temperature cycle. This procedure represents a very delicate phase and has a great influence on the final signal quality. Indeed, if non

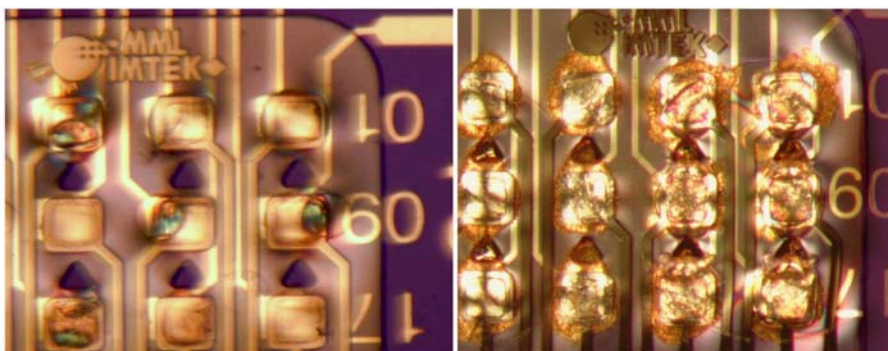


Fig. 3. Detail of chip/cable bonding areas. When overpressure is occurring, the contact material might exit the contact area and create shortcuts (as on the right picture).

optimal pressure or temperature parameters are chosen, the leads material might exit the contact areas and create short circuits and cross-talking between two non communicating contacts. When this happens, the final signals of the involved sensors might be compromised or affected by high basic noise. To verify the good functioning of the sensors, the resistances of all the contacts have been tested before the implementation of the chip. Typical values of some $k\Omega$ are characteristic of communicating contacts, while no resistance should be measured between non communicating contacts. In Fig. 3 two different bonding areas are presented. On the left an example of a correctly bonded cable is given, while on the right the result of an overpressure during the bonding phase is shown. In the first case, the recorded signals presented smaller values of basic noise compared to the ones from the chip on the right.

3 Sensors calibration and preliminary results

The calibration of the sensors is divided in two phases. At first the thermistors are calibrated using the thermocouples (Type K, NiCr-Ni) on the heating unit as reference. As a second step, the thermopiles are calibrated using the thermistors on the chip as reference.

3.1 Calibration of the RTD on the chip

The thermistors are calibrated without a gas flowing in the microchannels. This allows considering that, at steady state, the sensor layer, the test section and the copper blocks reach the same temperature. Different set points have imposed with the controlled channels of the power station, heating the copper blocks. The ranges for the temperature set points have been chosen within the limits encountered for the mechanical stability of the chip. The chip has been heated up to about 350 K without major fractures occurring. However, a confidence interval from ambient temperature up to 330 K has been chosen for the calibration. The relative fragility of the chip is not connected to the materials

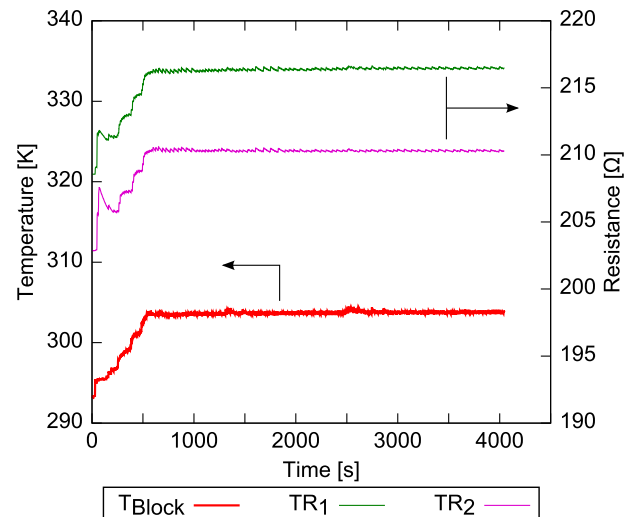


Fig. 4. Example of signal from two thermistors with reference temperature set at 303 K (red curve).

themselves, which on the contrary could stand higher temperatures, but is rather related to the mechanical and thermal stresses occurring during the tests. The whole chip structure is indeed relatively large and presents several points for crack growth, especially in correspondence of the membranes. For these reasons, particular attention should be paid during the mounting of the chip on the PTFE recess, and during the device assembly. Sudden thermal stresses together with severe pressure gradients along the chip should also be avoided. A possible solution for this problem could be the design of several small chips containing one membrane each and distributed along a support frame. However, in

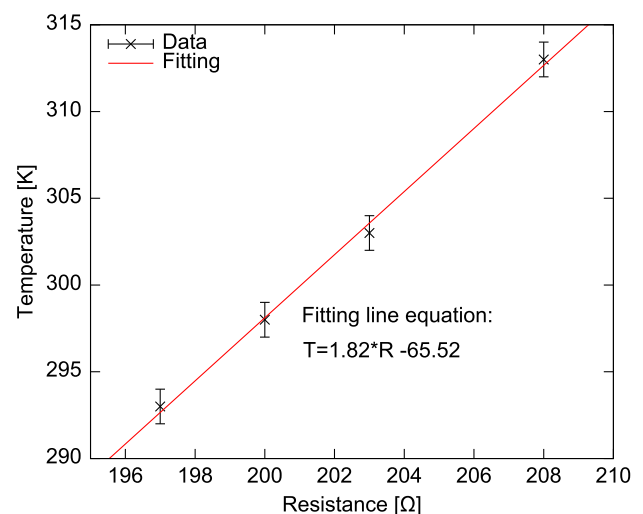


Fig. 5. Calibration fitting for a thermistor.

this case leakage issues and non uniformity of the surface could be encountered. As the main interest of the experimental campaign is the study of surface effects, the authors preferred on a first stage limiting the temperature window, but keeping a relatively uniform wall surface. New configurations could be tested in the future to increase the allowable temperature ranges.

Once the steady state is reached, the reference signal of the thermocouples and the resistance signals from the RTD sensors are recorded. Finally, for each set point the average values of the reference block temperature and of the corresponding resistance are calculated. These results are reported on a resistance-temperature plot, where, with a least square fitting method the calibration coefficients for each sensor are calculated.

In Figure 4 the recorded signals of one heated block and two corresponding thermistors (as example) are shown for a temperature set point of 303 K. From the plots it is evident that the sensors presents a good time response to temperature changes (they signal shapes follow well the temperature reference behavior), and have also a good time stability (no drift in time).

Figure 5 presents an example of calibration fitting for one thermistor. A good linear behavior in the tested temperature window has been retrieved for all the thermistors.

Tab. 1. Calibration coefficients for the tested thermistors.

Sensor	Fitting coefficients		Total error
TR1	2.36	-241.46	± 1.53 K
TR2	1.91	-153.44	± 1.25 K
TR3	1.67	-71.07	± 1.10 K
TR4	1.44	-8.13	± 1.35 K
TR5	2.02	-100.98	± 1.20 K
TR6	1.81	-70.11	± 1.12 K
TR7	1.89	-81.17	± 1.13 K
TR8	1.52	-15.99	± 1.30 K

Table 1 reports the final calibration coefficients for the tested thermistors. The indicated uncertainties for each sensor have been calculated taking into account three main error sources: the uncertainty associated to the temperature reference, the uncertainty associated to the fitting approximation and the calibration uncertainty associated to the error of the resistance measurement (calculated with the propagation error theory starting from the linear relation between temperature and resistance).

3.2 Calibration of the thermopiles

For the calibration of the thermopiles it is necessary to establish a controlled temperature difference across the membranes. The procedure has been performed with a high flow rate of gas flowing inside the microchannel, while the copper blocks have been heated to a defined set temperature. The high velocities reached by the gas allow considering the flow heating throughout the channel negligible. Therefore it is possible to assume the temperature difference between the gas and the chip constant all along the structure. To verify this point the gas inlet and outlet temperatures have been monitored during the tests.

The first results obtained with this procedure showed that the recorded signals were affected by high levels of noise, presenting non periodic and non symmetric amplitude oscillations. This results mainly from the cross talking between the different contact on the bonding area. An amplitude average analysis has been implemented with MATLAB® allowing the filtering out of the basic noise and the insulation of the signal related to the temperature difference across the chip.

In Fig. 6 an example sequence is shown where, starting from a situation of no temperature difference across the membrane, a sudden temperature step is established on the copper block, and a corresponding step in the average value of the thermopile voltage is detectable. As for the thermistors, the integrated sensors show a very good time response in answer to temperature changes.

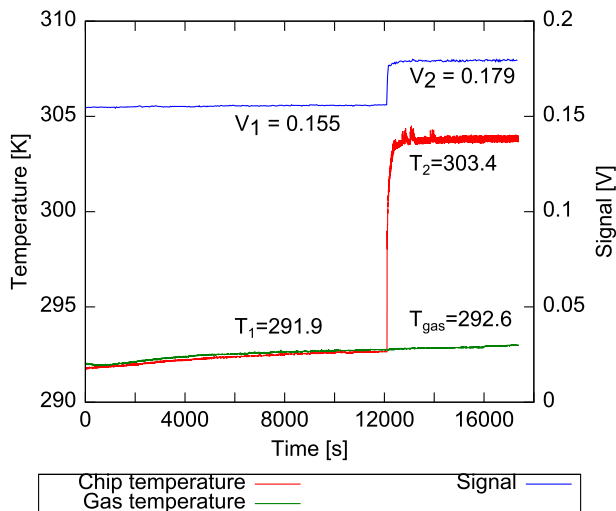


Fig. 6. Example of thermopile signal after the amplitude filtering for the elimination of the basic noise.

For the calibration to be completed a series of set points should be imposed and the calibration fitting should be calculated. However, to retrieve more precise results it has been decided to implement new chips, which have been prepared with particular attention to the bonding phase. Optimized temperature and pressure parameters have been found allowing better bonding conditions and an overall reduction of the interactions between adjacent contacts. These new chips showed good preliminary results and a better behavior of the thermopiles (i.e. reduced basic noise influence) is expected too.

4 Conclusions

This work presented a new integrated MEMS-based sensor system for the online measuring of temperature. The designed sensors allow a reduced flow disturbance and therefore are particularly indicated for microflow studies. Differently from already proposed configurations, the developed setup does not limit the use of structure materials to those compatible with silicon fabrication technologies, but allows the integration and the exchange of different tests structures which can be manufactured in principle from any material (e.g. metals, polymers and ceramics).

The preliminary tests with the prototypes showed overall good results in term of

sensitivity, time response and stability. Optimization is still needed to reduce the noise influence on the signals, and to improve the mechanical stability of the chip. New configurations could also be tested, after the first experimental campaign.

The present design has been developed for the study of the gas wall interactions of rarefied gases in microchannels. However, as it does not require particular adaptation techniques for the assembly, the system can be easily used for a series of different applications where in situ analysis is of advantage. Moreover, possibilities for integration with active actuating layout are also foreseen. The proposed system constitutes a step forward in the state of the art for integrated miniaturized sensing technologies from application-tailored designs to flexible multitasking ones. New possibilities for a broaden development and implementation of these systems is foreseen by the authors.

Acknowledgments

The research leading to these results has received funding from the European Community's Seventh Framework Program (FP7/2007-2013) under grant agreement n° 215504.

The authors wish to acknowledge Dr. Patrick Ruther from IMTEK, University of Freiburg, for his work and cooperation in the design and fabrication of the integrated microsensors.

References

- Arklic, E. B., Breuer, K. S., Schmidt, M. A., 1994. Gaseous flow in microchannels. In: ASME. Application of Microfabrication to Fluid Mechanics. Vol. FED-197, pp. 57-66.
- Beskok, A., Karniadakis, G. E., 1999. A model for flows in channels, pipes, and ducts at micro and nano scales. *Microscale Therm. Eng.*, 3(1), pp. 43-77.
- Colin, S., 2005. Single phase gas flow in microchannels. In: S. G. Kandlikar, ed. Heat transfer and fluid flow in minichannels and microchannels. Elsevier Science. Ch. 2.
- Gad-el-Hak, M., 2001. Flow Physics. In: M. Gad-

- el-Hak, ed. The MEMS Handbook. CRC Press. Ch. 4.
- Guo, Z. Y., Li, Z. X., 2003. Size effect on single-phase channel flow and heat transfer at microscale. *Int. J. Heat Fluid Fl.* 24, pp. 284-298.
- Ko, H. S., Gau, C., 2009. Bonding of a complicated polymer microchannel system for study of pressurized liquid flow characteristic with the electric double effect. *J. Micromech. Microeng.* 19, paper No. 115024.
- Krause, L. N., Fralick, G. C., 1977. Miniature drag force anemometer. NACA Technical Memorandum, X-3507.
- Maikowske, S., Brandner, J. J., Lange, R., 2010. A novel device for the optical investigation of phase transition in micro channel array evaporators. *Appl. Therm. Eng.* 30, pp. 1872-1876.
- Morini, G. L., 2004. Single-phase convective heat transfer in microchannels: a review of experimental results. *Int. J. Therm. Sci.* 43, pp. 631-651.
- Park, H., Pak, J. J., Son, S. Y., Lim, G., Song, I., 2003. Fabrication of a microchannel integrated with inner sensors and analysis of its laminar flow characteristics. *Sensor Actuat. A-Phys.* 103, pp. 317.
- Pitakarnop, J., Varoutis, S., Valougeorgis, D., Geoffroy, S., Baldas, L., Colin, S., 2010. A novel experimental setup for gas microflows. *Microfluid. Nanofluid.*, 8, pp. 57-72.
- Rosa, P., Karayiannis, T. G., Collins, M. W., 2008. Review of heat transfer in microchannels. In *Proc. 1st European Conference on Microfluidics, μ Flu08-27.*
- Schmidt, M. A., Howe, R. T., Senturia, S. D., Haritonidis, J. H., 1988. Design and calibration of a microfabricated floating-element shear-stress sensor. *IEEE Transactions on Electronic Devices* 35, pp. 750-757.
- Turner, S. E., Lam, L. C., Faghri, M., Gregory, O. J., 2004. Experimental investigation of gas flow in microchannels. *J. Heat Transf.*, 126, pp. 753-763.
- Van Herwaarden, A. W., van Duyn, D. C., van Oudheusden, B. W., Sarro, P. M., 1989. Integrated thermopile sensors. *Sensor Actuat. A-Phys.* 23, pp. 621-630.
- Van Oudheusden, B.W., 1988. Silicon flow sensors, *IEE Proceedings* 135 (5), pp.373-380.
- Vittoriosi A., Brandner, J.J., Dittmeyer, R., 2010. Gas wall interactions of rarefied gases in MEMS: a new experimental device with integrated sensors. In *Proc. 8th International Conference on Nanochannels, Microchannels and Minichannels*, Paper No. FEDSM-ICNMM2010-30488.
- Wu, S., Mai, J., Zohar, Y., Tai, Y. C., Ho, C. M., 1998. A suspended microchannel with integrated temperature sensors for high pressure flow studies. In: *IEEE, 11th International Workshop on Micro Electro Mechanical Systems*. Piscataway, NJ.
- Xue, Z., Qiu, H., 2005. Integrating micromachined fast response temperature sensor array in a glass microchannel. *Sensor Actuat. A-Phys.* 122, pp. 189-195.